

Experimental Characterisation of Cure-Dependent Spring-Back Behaviour of Metal-Composite Laminates in a Hot-Pressing Process

Liu, Shichen; Sinke, Jos; Dransfeld, Clemens

DOI

[10.1007/s10443-024-10266-5](https://doi.org/10.1007/s10443-024-10266-5)

Publication date

2024

Document Version

Final published version

Published in

Applied Composite Materials

Citation (APA)

Liu, S., Sinke, J., & Dransfeld, C. (2024). Experimental Characterisation of Cure-Dependent Spring-Back Behaviour of Metal-Composite Laminates in a Hot-Pressing Process. *Applied Composite Materials*, 32(1), 173-198. <https://doi.org/10.1007/s10443-024-10266-5>

Important note

To cite this publication, please use the final published version (if applicable).
Please check the document version above.

Copyright

Other than for strictly personal use, it is not permitted to download, forward or distribute the text or part of it, without the consent of the author(s) and/or copyright holder(s), unless the work is under an open content license such as Creative Commons.

Takedown policy

Please contact us and provide details if you believe this document breaches copyrights.
We will remove access to the work immediately and investigate your claim.



Experimental Characterisation of Cure-Dependent Spring-Back Behaviour of Metal-Composite Laminates in a Hot-Pressing Process

Shichen Liu¹ · Jos Sinke¹ · Clemens Dransfeld¹

Received: 5 June 2024 / Accepted: 30 August 2024
© The Author(s) 2024

Abstract

This study focuses on the spring-back as a function of the degree of cure on single-curved metal-composite laminates. The manufacturing through a hot-pressing process involves different (curing) stages and can reduce the spring-back with the proper combination of forming and curing. The cure-dependent spring-back is measured and analysed as a function of material constituents, fibre directions, laminate layups, and the process parameters including temperature, holding time and pressure. The results demonstrate that the spring-back ratio after full-cured process is relatively small and mainly depends on the mechanical properties of the metal sheet in laminates. However, temperature and time have a significant effect on the spring-back of partially-cured laminates and the same type of fibre prepreg combined with two different metal sheets have similar trends of spring-back reduction. Moreover, the study found that the hybrid laminates with aluminium sheet delaminate at low pressure after full-cured, while the delamination disappears as the pressure increases. The characterisation on cure-dependency of the spring-back contributes to a better understanding of the deformability of the metal-composite laminates during the hot-pressing process and offers an opportunity to tune the spring-back of these laminates.

Keywords Metal-composite laminates · Cure-dependent spring-back · Laminate design · Degree of cure · Hot-pressing

1 Introduction

Hybrid metal-composite laminates are high-performance lightweight materials consisting of thin metal sheets and fibre reinforced polymers by alternatively stacking, curing under proper temperature and pressure [1, 2]. These hybrid materials combine the advantages of metal sheet and fibre reinforced polymer like high specific strength and stiffness, and other

✉ Shichen Liu
S.Liu-7@tudelft.nl

¹ Faculty of Aerospace Engineering, Delft University of Technology, Delft, The Netherlands

excellent properties like high fatigue and impact resistance, as well as the better corrosion and fire resistance, etc. [3–6]. However, the manufacturing process of such hybrid laminates is difficult as various forming and curing stages are required coupled with complex deformation and failure modes [7–9]. To improve the manufacturability of the hybrid laminates, an integral forming and curing cycle is proposed in Fig. 1. The most critical stages in the process are preheating and curing of the laminates before and after hot-pressing process. The time and temperature need to be controlled in the preheating stage, so that the inter-ply slip at the metal-prepreg interfaces and the intra-ply shear within the prepregs can be greatly enhanced when the resin viscosity decreases [10–13]. The hybrid laminate is formed and cured in the subsequent stage, avoiding loading and unloading of the part and the use of an extra curing system, such as vacuum pump or autoclave, which can be time-saving and cost-saving [14]. In addition, there also arises some scientific questions on how the state of curing affects the spring-back and thereby the accuracy of the final part and whether the pressure applied during curing is relevant in reducing or eliminating the spring-back, which plays a role in the accuracy of the related tool geometry as well.

The concept of spring-back comes as a consequence of the elastic strain recovery after the removal of forming loads. In the conventional sheet metal forming process, the occurrence of spring-back is common and inevitable in each stage where the metal material undergoes plastic deformations. The parameters affecting the spring-back behaviour of metal sheets are mainly related to the stresses generated during the loading and unloading process and can be divided into three groups: material, tool and process related geometry. The properties of the metal sheet such as size and thickness, elastic modulus, yield strength and hardening coefficient, affect the elastic spring-back during forming. For example, the material with a higher yield strength will have a higher ratio of elastic-plastic strain for equivalent elastic moduli, while the metal sheet with a higher elastic modulus shows less spring-back than a material with a lower elastic modulus for equivalent yield strengths [15–17]. For the geometry related parameters, the punch height and radius, die opening and radius, the tool-metal friction are all critical variables affecting the spring-back [18–20]. Gawade et al. [19] found that the metal spring-back is minimum up to a certain value of the die radius to sheet thick-

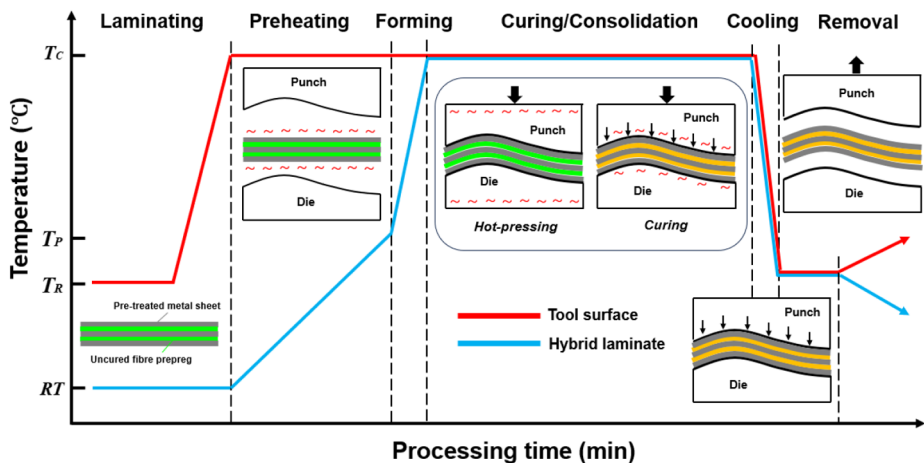


Fig. 1 Schematic graph on the processing temperature-time profile for the tool surface and hybrid laminate in an integral forming and curing cycle

ness ratio and it increases with the increase in such R/t ratio. In addition, the reduction in friction between the metal sheet and forming tools increases the spring-back and decreases the bend force. Other critical factors influencing the spring-back of metal sheet are the process parameters like the forming rate and blank holder force, as well as the temperature and quenching treatment, etc. Melwin et al. [21] also found that the spring-back decreases with an increase in cooling rate for a hot stamping steel and the increase in cooling rate results in spring-forward owing to the formation of an increased volume fraction of martensite.

The spring-back behaviour of fibre reinforced polymers also originates from three different mechanisms: chemical mechanism, thermo-mechanical mechanism and the interactions between the tool and the composite laminate [22–32]. While the properties of the fibre materials remain essentially constant, the resin properties change dramatically during the cure cycle as it polymerizes and crosslinks transitioning from a viscous to rubbery and finally glassy state. Therefore, the resin morphology results in a volume change, which causes the accumulation of internal stress. With the increase of such internal stress which induces changes in curvature in plates, the spring-in phenomenon due to this chemical shrinkage cannot be ignored [22]. The thermo-mechanical mechanism is mainly due to the physical and mechanical differences between the fibres and the polymeric matrix. The coefficient of thermal expansion (CTE) of polymer-matrix materials is usually much higher than that of the fibres as the CTEs of many fibres are orthotropic. This results in residual stresses existing on a micro-mechanical level for the unidirectional materials during processing. These residual stresses can affect the stress-strain behaviour and failure which influence the spring-back. Brauner et al. [26, 27] developed a simulation tool for the analysis of residual stresses related to the resin transfer moulding process, and a visco-elastic material model was derived integrating a dependency of the time-temperature-polymerisation and fibre volume content on the stress relaxation behaviour. In addition, the mechanical properties of the resin depend on the degree of cure which can be used to evaluate the development of spring-back. Uriya et al. [28] studied the spring-back behaviour of a carbon fibre-reinforced plastic sheet after cold and warm V-bending test and found a large amount of decrease in spring-back when the forming temperature and degree of cure increases. Also, Pereira et al. [29] showed that a polymer with a lower degree of cure has a lower modulus of elasticity than a fully-cured polymer and the degree of cure associated with the cooling rates influences the spring-back. The third mechanism of spring-back is due to the contact effects between the metallic tool and the composite part. The parameters like tool material, surface condition (friction), cure cycle and pressure are shown to have a significant effect on the spring-back [30–32].

The mechanisms and factors affecting the spring-back behaviour of metal sheet and fibre reinforced polymer apply to the hybrid metal-composite laminates as well [33–41]. The amount of spring-back in such laminates depends on the material parameters such as the material constituents, the laminate layup and thickness, as well as the fibre orientations. Keipour et al. [35] performed an experimental and numerical study of the spring-back in a hat-shaped bending test of a 2/1 fibre metal laminate and found that the thickness of composite core had limited effect on spring-back when the elastic modulus of the core is lower than the metal skin. However, Isikatas et al. [36] found that the amount of spring-back in a hybrid 2/1 laminate decreases with the increase of the thickness of the composite core when combining the aluminum 5754-H22 sheet and carbon fibre-reinforced plastics by adhesive. In addition, many scholars found that the spring-back differs on the processing

parameters under various manufacturing processes. Kim et al. [39] considered a brake forming process for fabricating the fibre metal laminate stringers and examined the spring-back under different processing conditions. They discovered that the spring-back ratio increases linearly with increase of punch radius while the spring-back ratio increases rather slowly with the increasing punch speed at room temperature. Also, the increase of forming force from 500 N to 5000 N with a heat-up temperature of 100°C results in a significant decrease on spring-back. Vahid et al. [40] focused on the spring-back behaviour of the PVC-based metal-composite laminates under press forming conditions and concluded that laminate stretching is the main deformation mechanism at low temperatures which results in high spring-back, while the increase of forming temperature activates the laminate-sliding mechanism and leads to the spring-back reduction. Safari et al. [41] conducted an experimental assessment of the creep forming properties of fibre metal laminates and studied the effect of temperature and time on spring-back. The result validated that the spring-back of the creep-formed laminates decreases with an increase in either time or temperature due to the decrease of elastic strain and the increase of creep strain. Besides, they believed that through multi-objective parameter optimisation during the forming process of the metal-composite laminates, the minimum spring-back can be achieved. Saadatfard et al. [42] and Blala et al. [43] studied the hydromechanical forming of metal-composite laminates and found that blank holder force and fluid pressure play an important role on the defect and failure of the final product including spring-back.

Therefore, due to the high spring-back of the cured hybrid laminate, the in-situ curing of the curved shape after forming process of uncured laminate becomes a trend. However, the role of individual metal sheet and prepreg layers in an uncured laminate during forming is unknown. Also, how the degree of cure and the forming pressure affect the interaction at the metal-composite interfaces remains to be discussed. Besides, there is a lack of studies on quantifying the laminate spring-back as a function of degree of cure and the experimental methods for the selection of appropriate material constituent and processing parameters for laminate forming with uncured prepreps have not been proposed.

The main idea of this work is to investigate the effects of spring-back of hybrid metal-composite laminate under the proposed hot-pressing process. Two processing conditions of full-cured and partially-cured after the bending of “wet” (uncured) hybrid laminates are characterized by comparing variations of the calculated spring-back ratios. A series of experiments are performed to work on the effect of laminate design and processing parameters on the spring-back behaviour of such hybrid materials. The study aims to evaluate the factors affecting the cure-dependent spring-back of metal-composite laminate as those effects are mutually-related. The test characterisations are performed to explore which mutual correlations are the most important and how they affect the final prediction of spring-back. Then, the cure-dependent spring-back behaviour of the metal-composite laminates can be optimized and controlled to make more accurate products.

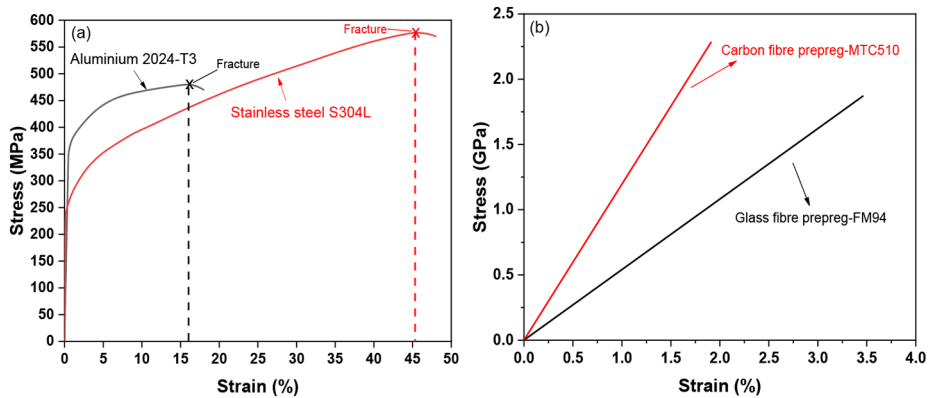


Fig. 2 Engineering stress-strain curves of the materials used for the spring-back analysis: **(a)** Metal alloys; **(b)** Fibre prepregs

Table 1 Mechanical properties of the material constituents in hybrid laminates [44, 45]

Materials	Density (g/cm ³)	Elastic modulus (GPa)	Pois- son's ratio	Shear modu- lus (GPa)	Yield strength (MPa)	Ultimate strength (MPa)	Shear strength (MPa)	Elonga- tion at break (%)
Aluminium alloy 2023-T3	2.7	71	0.33	28	320	480	283	16.2
Stainless steel 304 L	8.0	200	0.30	77	210	574	378	45.6
UD glass fibre prepreg-FM94	2.6	54.0/9.4	0.33	5.5/2.6	-	1870/50	38.5	3.8
UD carbon fibre prepreg-MTC510	1.5	119.3/8.2	0.34	3.6/2.0	-	2282/54	99	1.3

2 Materials and Methods

2.1 Material Constituent

The raw materials used for the laminate preparation are metal sheets of aluminium alloy 2024-T3 and stainless steel 304 L, as well as two different fibre prepregs. The surfaces of aluminium sheet were anodized by phosphoric acid and both metal materials with the thickness of 0.5 mm were washed by acetone [1, 2]. The engineering stress-strain curves which exhibit the elastic-plastic performance of the metal alloys used in the test are shown in Fig. 2(a) and these can illustrate the effect of metal behaviour on spring-back. For the two fibre-reinforced prepreg systems, a unidirectional S2 glass fibre-FM94 epoxy prepreg with a nominal thickness of 0.18 mm as well as a T300 carbon-MTC510 UD prepreg with a nominal thickness of 0.15 mm were selected. The fibre volume fraction for both prepregs was 60% and the thermoset polymers were cured at the temperature of 120°C and pressure of 6 bar which follows a standard curing cycle [44, 45]. The mechanical properties of the material constituents in hybrid laminates are presented in Table 1 and the behaviour of the metal sheet cannot be affected under the investigated temperature ranges. Two parameters

of the elastic modulus and ultimate strength for UD prepregs represent the properties in fibre orientation of 0° and 90° , respectively. For all tests, the rolling direction for the metal sheet and the fibre orientation of 0° for the fibre reinforced prepreg are parallel to the bending line of the laminate.

2.2 Rheological Analysis

FM94 and MTC510 are two temperature-dependent epoxy systems allowing compatibility for metal sheet bonding of the metal-composite laminates. For the hot-pressing process of the prepared and uncured blanks, the degree of cure and thereby the resin viscosity of the epoxy plays a critical role in the relative sliding between the interlayers and the occurrence of possible defects like fibre buckling. In order to obtain the relationship between the degree of cure and resin viscosity, Differential Scanning Calorimetry (DSC) and rheometer analysis can be used for the characterisation of cure kinetics and rheokinetics, respectively [44, 46]. For DSC, the heat flow is the internal heat, H , generated per unit mass and per unit time during the cross-link reaction and is represented as:

$$\frac{dH}{dt} = H_{tot} \frac{d\alpha}{dt} \quad (1)$$

H_{tot} is the total heat of reaction after complete consolidation of the epoxy and α is the degree of cure. The cure rate and total heat of the reaction can be determined by iso-conversion DSC measurements where the resin is heated with a constant heating rate and the energy input is measured versus the cure time [47]. For the calculation of cure rate, the Kamal-Sourour reaction ratio equation [48] is proposed and fitted as follows:

$$\frac{d\alpha}{dt} = k_0 e^{(-EA/RT)} \alpha^m (1 - \alpha)^n \quad (2)$$

where R is the universal gas constant and T is the cure temperature in Kelvin, EA is the activation energy, k_0 is a coefficient and m, n are two fitting constants. The degree of cure α of the epoxy at any time t is calculated through the integration of the instant cure rate as:

$$\alpha(t) = \int_0^t \frac{d\alpha}{dt} dt \quad (3)$$

By using the kinetic model in Eq. (2) and fitted parameters obtained from Table 2, the degree of cure of the epoxy can be predicted for isothermal cure and the development of degree of cure under specific temperatures of the FM94 and MTC510 epoxy are presented

Table 2 Cure kinetic parameters for epoxy FM94 and MTC510 [47–49]

Parameter	FM94	MTC510
$k_0(1/s)$	3.52E+06	5.64E+06
$EA(J/mole)$	6.75E+04	6.21E+04
$m(-)$	0.558	0.314
$n(-)$	2.508	1.216
$H_{tot}(J/g)$	134.9	321.8

Fig. 3 Predicted degree of cure evolution of the epoxy under specific temperatures: Solid line-FM94 and Dashed line-MTC510

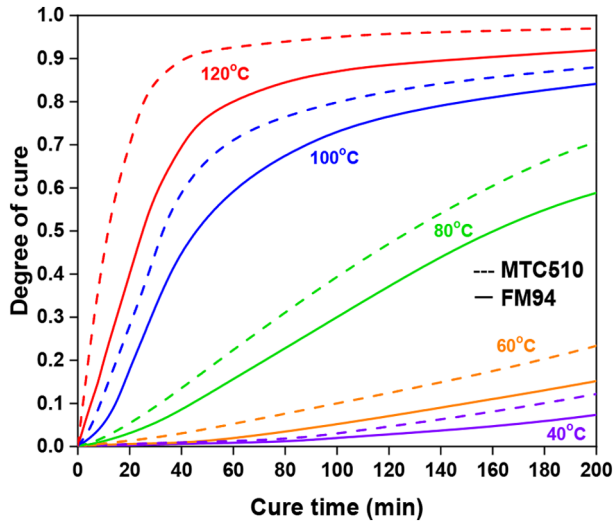
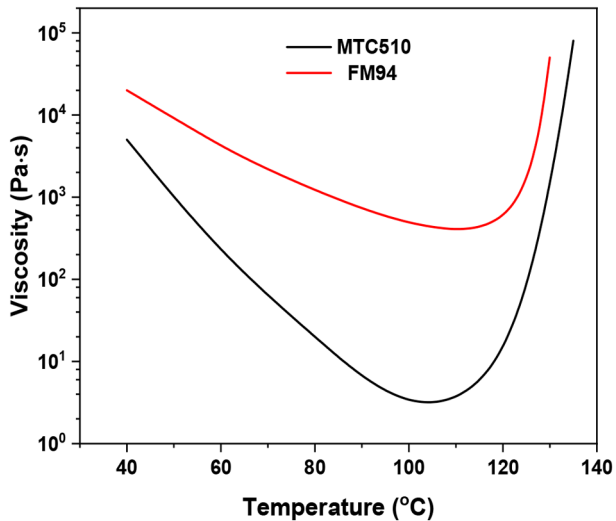


Fig. 4 Rheological data of the FM94 and MTC510 epoxy at the ramp of 2°C/min



in Fig. 3 [47–49]. The viscosity of the epoxy evolves as a function of temperature and time: $\eta = f(T, t)$, or degree of cure and temperature: $\eta = g(T, \alpha)$. The rheological behaviour of the FM94 adhesive and MTC510 epoxy at a ramp of 2°C/min as provided by the material suppliers [44, 45] are presented in Fig. 4.

2.3 Experimental Setup

The hot-pressing process which can be an alternative approach of forming metal-composite laminate was performed on a 1000kN heated flat Joos Press machine. In order to investigate the influence of spring-back without the forming defects like metal wrinkling or fibre buckling, a single-curved mould with the size of 250×120×150 mm was designed and manu-

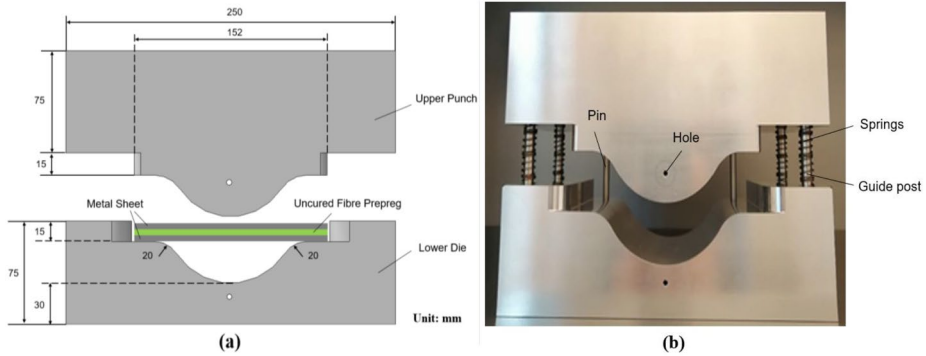


Fig. 5 Single-curved mould design for the laminate hot-pressing process: (a) mould dimension; (b) mould manufacture

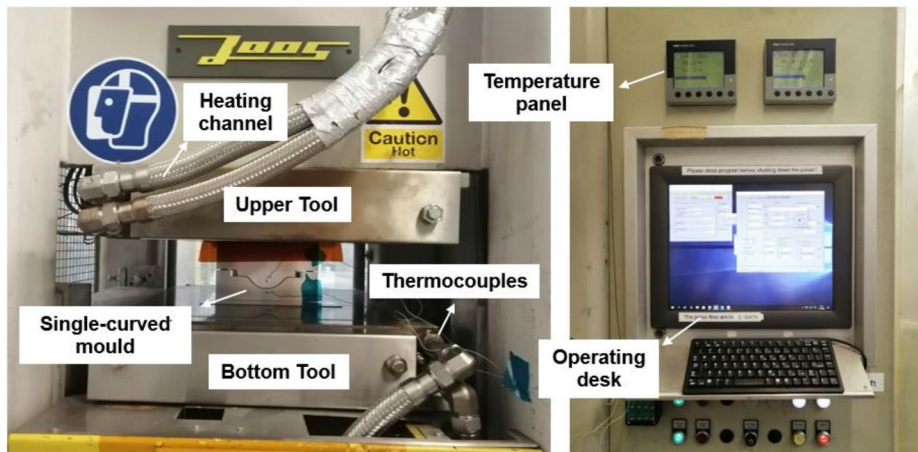


Fig. 6 Experimental setup and apparatus for the hybrid laminate hot-pressing process

factured, as shown in Fig. 5. Four spring-wrapped guide posts were made to control the movement of the upper mould and ensure that the tool returns to its original position when the pressure is released. The specimen with initial dimensions of 150×40 mm was placed into the mould and positioned by two long vertical pins on the back. The experimental setup and apparatus for the laminate hot-pressing process is exhibited in Fig. 6. The temperature of upper and lower tool of the press was set at about 40°C (T_R) and gradually goes up to the curing temperature of 120°C (T_c) before preheating process of the laminates. The real-time temperature in the mould was recorded by the thermocouples in holes in the upper and lower tools, and displayed on the temperature panel. The experimental forming cycle includes a temperature rise from room temperature (RT) to the preheating/forming temperature (TP) at a rate of $2^\circ\text{C}/\text{min}$ and the forming pressure to the set value gradually increased to the increasing temperature. Then, after maintaining a closed mould for a certain period of time, the temperature is reduced to the reset temperature (T_R) at a cooling rate of $4^\circ\text{C}/\text{min}$. For

Table 3 Material configurations used for hot-pressing process

Structure	Material configuration		
Metal sheet	Aluminium 2024-T3	Stainless steel 304 L	
Fibre preperg (UD)	S2 glass-FM94	T300 carbon-MTC510	
Laminate layup	2/1	3/2	4/3
Fibre orientation	0°/0°	0°/90°	90°/90°

Table 4 Test conditions used for laminate hot-pressing process

Test Parameter	Baseline value	Additional values investigated
Temperature (°C)	80	40, 60, 100, 120
Holding time (min)	20	0, 10, 30, 120
Pressure (bar)	6	0.1, 1, 10, 20

Table 5 Computed degree of cure used under different holding time and temperature

Degree of cure	Carbon Fibre Prepreg-MTC510			Glass Fibre Prepreg-FM94		
Temperature (°C)	10 min	20 min	30 min	10 min	20 min	30 min
40	0.002	0.005	0.009	0.001	0.002	0.005
60	0.008	0.012	0.020	0.003	0.006	0.013
80	0.016	0.047	0.096	0.011	0.029	0.058
100	0.121	0.285	0.467	0.052	0.184	0.363
120	0.452	0.706	0.854	0.208	0.415	0.589

the setup, it was possible to adjust the process parameters of forming temperature, holding time and forming pressure as they may affect the spring-back.

Table 3 presents the material configurations used for the hot-pressing process and Table 4 shows the test conditions for the experiments. The test varies one parameter at a time while keeping the other parameters at their baseline values. For each configuration under these test conditions, at least three specimens are tested. Among all the investigated test conditions, the hybrid laminates are regarded as complete cured when the forming temperature reaches 120°C with a holding time of 120 min and forming pressure of 6 bar. However, the tests performed below these temperature and time conditions are considered as partially-cured. As the temperature and time characterise the evolution of degree of cure, the value obtained from the rheological analysis is used to investigate the effect on the cure-dependent spring-back. The computed degree of cure for the prepreps under the selected temperature and time summarised in Table 5 assumes isothermal conditions and do not account for the transient heating phase when the material is initially placed in the mould. Besides, the laminate is assumed to be full-cured once the degree of cure exceeds 0.9 and the cure is not assumed to begin when the degree of cure is less than 0.01. The schematic graph of the laminate forming process is presented in Fig. 7 where the spring-back behaviour is compared for partially-cured and full-cured conditions.

2.4 Spring-back Characterisation

In the traditional metal sheet forming process, the spring-back before and after unloading is mainly characterised by the spring-back angle $\Delta\theta$ and spring-back radius ΔR . As shown in Fig. 8, the forming angle of the metal sheet is $\theta()$, and the corresponding forming radius is

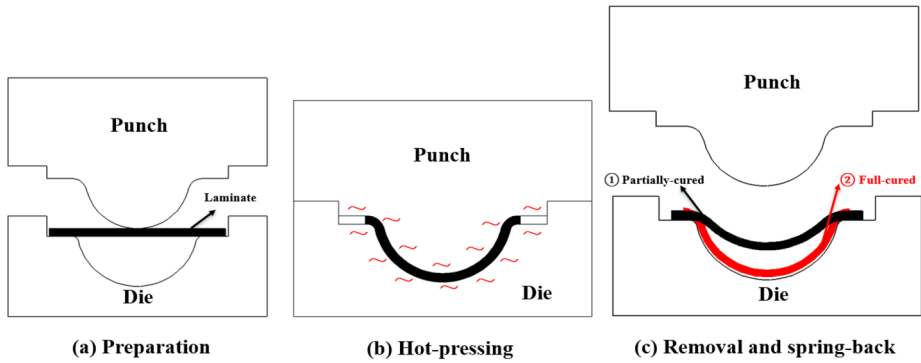


Fig. 7 Schematic graph of the laminate forming process on cure-dependent spring-back

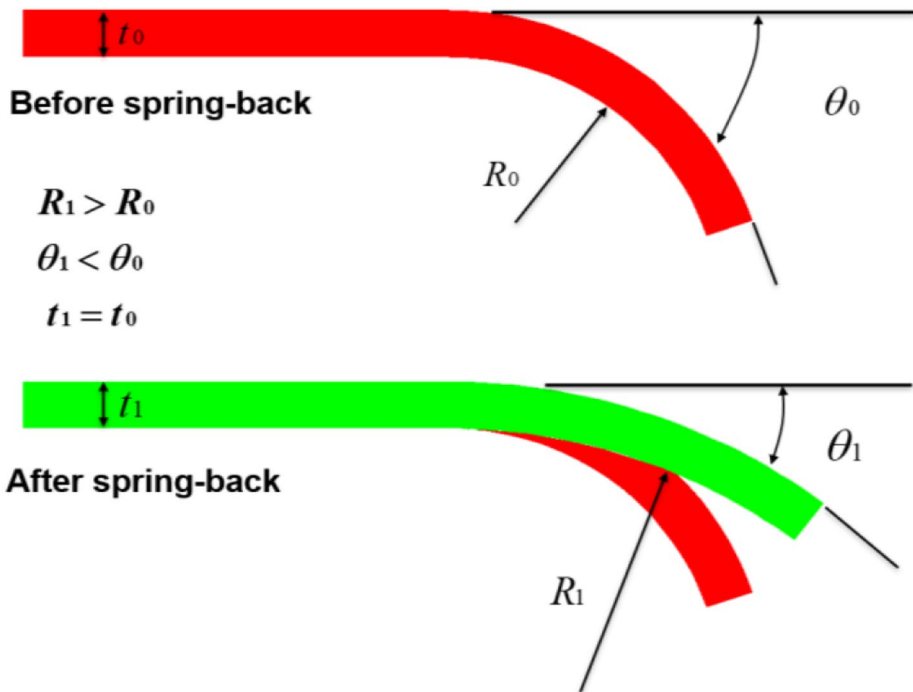


Fig. 8 Definition of the spring-back angle and radius for the metal sheet forming process

R_0 . After the spring-back, the value changes to θ_1 and R_1 , respectively. Then, the spring-back angle and radius are defined by Eqs. (4) and (5):

$$\Delta\theta = \theta_0 - \theta_1 \quad (4)$$

$$\Delta R = R_1 - R_0 \quad (5)$$

Here, R_0 and R_1 are both the radius of the neutral layer where the strain is assumed to be zero. During the spring-back period, it is assumed that the in-plane sections remain planar and the strain due to bending is proportional to the distance from the neutral layer. In addition, the through-the-thickness stress is ignored and no change occurs in sheet thickness ($t_0 = t_1$). Based on these assumptions, the relationship of forming angle and radius can be written as [36, 50]:

$$\theta_0 \cdot R_0 = \theta_1 \cdot R_1 \quad (6)$$

Then, the spring-back ratio K which can be defined as the variation of spring-back angle divided by the initial forming angle is expressed as:

$$K = \frac{\Delta\theta}{\theta_0} = 1 - \frac{\theta_1}{\theta_0} = 1 - \frac{R_0}{R_1} \quad (7)$$

For the hot-pressing of the single-curved laminate in this work, the geometrical analysis of the spring-back ratio after removal of the forming loads is showed in Fig. 9. The flange and inner fillet regions of the laminate exhibits non-cylindrical shape after spring-back which may affect the measurement of the forming depth and thus, influence the calculation of the spring-back radius. Therefore, a measured length L which is symmetrical to the vertical centreline is introduced to evaluate the spring-back behaviour. The geometric relations are expressed as follows:

$$\begin{aligned} (R_i - D_i)^2 + \left(\frac{L}{2}\right)^2 &= R_i^2, \\ R_i &= \frac{L^2 + 4D_i^2}{8D_i}, \quad i = 1, 2 \end{aligned} \quad (8)$$

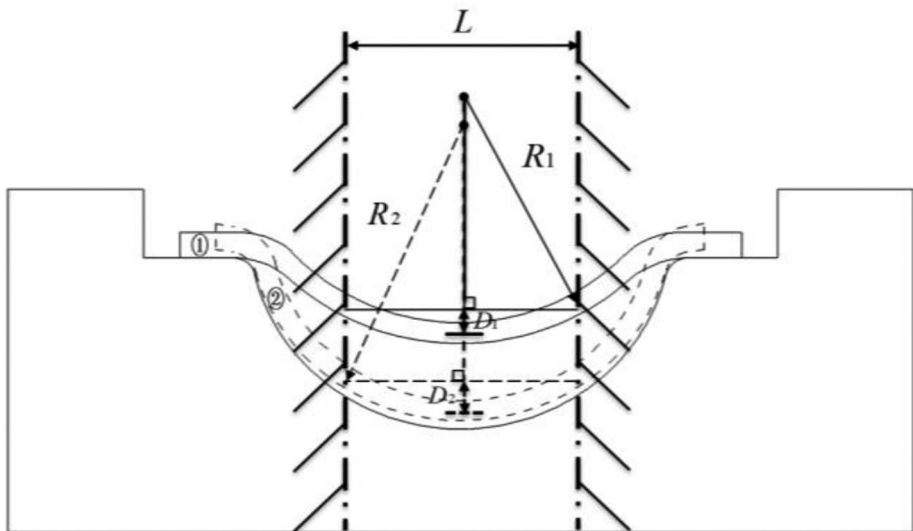


Fig. 9 Geometric analysis of the laminate spring-back radius after removal of the forming loads

where R and D are the formed radius and the geometric depth based on the measured length L , $i = 1, 2$ denotes the process conditions of partially-cured and full-cured, respectively. Here, the curvature under the measured length is assumed to be a constant value. In addition, the maximum geometric depth D_0 is 30 mm and the formed radius of the initial shape before spring-back R_0 is 50 mm. The dimensions are substituted into Eq. (8) and combined with Eq. (7) to obtain the spring-back ratio:

$$K_i = 1 - \frac{8DiR_0}{L^2 + 4Di^2}, \quad i=1, 2 \quad (9)$$

Therefore, the spring-back ratio under different curing conditions can be calculated once the geometric depth based on the measured length L is determined.

3 Results and Discussion

3.1 Effect of Measured Length on spring-back

For the hot-pressing process of single-curved semi-cylindrical parts with flange areas, the non-cylindrical shapes after spring-back affect the evaluation of the spring-back behaviour. In order to accurately obtain the value of formed radius associated with spring-back ratio, various measured lengths are applied for the measurement. The single-curved parts and their corresponding profiles by optical scanning after spring-back under various material combinations are shown in Fig. 10. The aluminium alloy (Al) and stainless steel (Ss) are the single-layer metal sheets, while the Al/GFRP and Ss/CFRP laminate with the layup of 2/1 and fibre orientation of $0^\circ/0^\circ$ are the hybrid materials under the conditions of full-cure. The spring-back profiles are sketched and placed into an identical coordinate system to measure D under different lengths as exhibited in Fig. 10. The formed radius can be calculated through the geometric relations in Eq. (8) and the measured length (L)-formed radius (R) curve is presented in Fig. 11. For the investigated hybrid laminates, there is not much difference in the calculated formed radius when the measured length is smaller than 80 mm. However, the formed radius increases as the length goes up to 90 mm and 100 mm. The increase of radius becomes more significant at smaller values of for the metal sheet especially for the single-layer aluminium 2024-T3. The results can be explained from the single-curved profiles in Fig. 10, since the larger length includes the flange and inner fillet regions, which may increase the final formed radius. Besides, the smaller geometric depth D exhibits more spring-back and allows more regions to be in the flange. Therefore, the shape after spring-back becomes non-cylindrical and the formed radius changes significantly. Based on the radius curves as function of the length for the different materials, the formed radius at the measured length of 60 mm is considered to be the optimum length for accurate formed radius determination.

3.2 Effect of Laminate Design on Spring-Back

The design of the metal-composite laminates consists of several material constituents, laminate layup and fibre orientation. After spring-back of the full-cured hybrid laminates, four

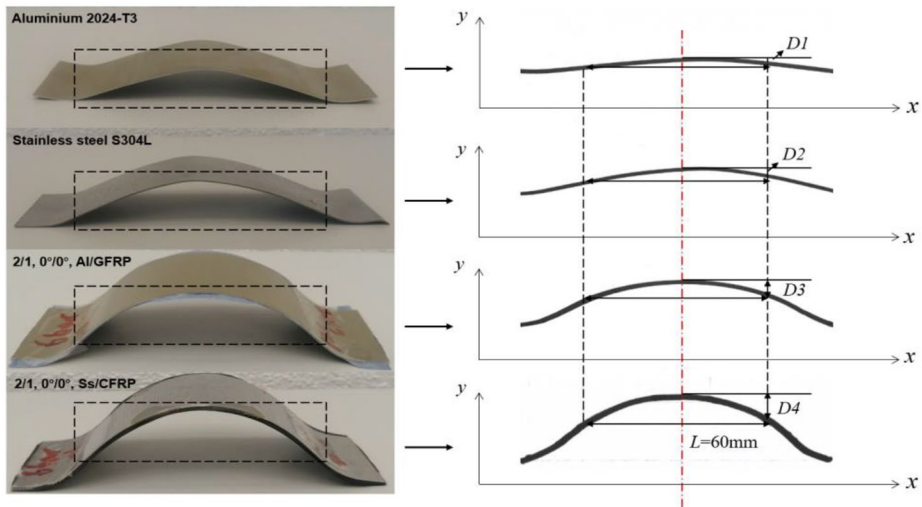
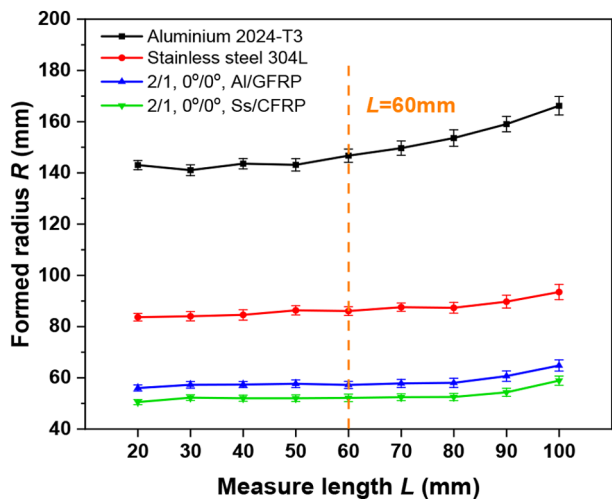


Fig. 10 Single-curved parts and their corresponding profiles after spring-back for various material combinations

Fig. 11 Evolution of formed radius under various measured lengths for different material combinations



different material combinations with the layup of 2/1 and fibre orientation of 0°/0° are shown in Fig. 12. It can be seen from the graph that the stainless steel with carbon fibre reinforced prepreg (Ss/CFRP) has the largest geometric depth at the optimum measure length and the geometric depth for the combination of aluminium alloy and glass fibre reinforced prepreg (Al/GFRP) is the smallest. Since the initial formed radius of the single-curved shape is 50 mm, a higher geometric depth after removal of the forming loads means a smaller spring-back ratio as the calculated formed radius is closer to the initial formed radius. Therefore, the result validates that the material constituents play a significant role in the spring-back of the metal-composite laminates. The relatively small spring-back behaviour of the hybrid laminates with stainless steel reveals that the overall spring-back behaviour is mainly influenced

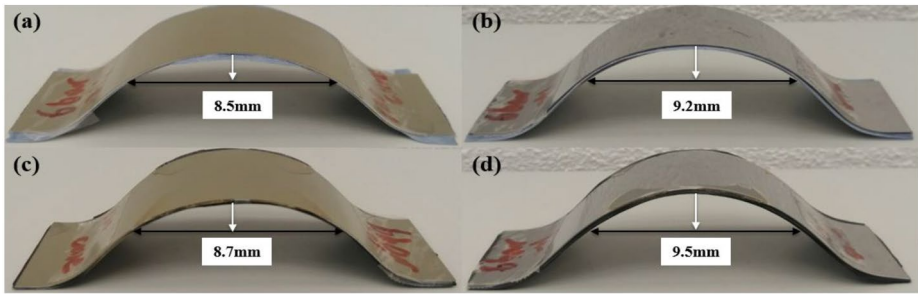


Fig. 12 Single-curved part after full-cured process with different metal-composite combinations: (a) Al/GFRP; (b) Ss/GFRP; (c) Al/CFRP; (d) Ss/CFRP

by the elastic-plastic deformation of the metal sheet. This can be explained from the stress-strain curve showed in Fig. 2, where higher elastic modulus and lower yield strength of the stainless steel result in a lower elastic response compared to the aluminium alloy as the metal sheet reaches the same amount of deformation. Besides, the hybrid laminates with carbon fibre prepreg have a small decrease on the spring-back after full-cured when compared with the metal-glass fibre reinforced hybrid laminates due to the higher elastic modulus and degree of cure (Fig. 3) for the metal-CFRP laminates. The result shown in Fig. 11 demonstrates that the presence of the prepreg system in hybrid laminate contributes significantly to the spring-back reduction when the laminate is full-cured. The calculated formed radiuses of the single-layer aluminium alloy and stainless steel after spring-back under the same conditions are 146.7 mm and 86.0 mm, and the spring-back ratios are 0.66 and 0.42, respectively.

The substantial spring-back reduction for the fibre metal laminates indicates that the spring-back is not only affected by the type of metal sheet as the aluminium alloy shows more spring-back than stainless steel, but also by the design of the laminate. As the schematic diagram of the laminate stress distribution before and after spring-back exhibited in Fig. 13, the bending deformation for metal sheet considers a material exhibiting elastic-ideal plastic behaviour without hardening. For the uncured hybrid laminate, the stress distribution for the metal sheet is symmetrical along the neutral layer, where the metal surfaces 1&2 (3&4) undergo the maximum tensile stress and compressive stress, respectively. In the outer metal surfaces, the stress will be capped at the maximum value where the vertical lines denote the plastic deformation regions. When a 2/1 laminate is bent with an uncured fibre prepreg in the middle (Fig. 13(a)), the metal sheets can spring-back (more or less) independently from each other after unloading. The inner surfaces (2&3) of the metal sheet slip over the uncured prepreg and this fibre prepreg does not offer any resistance to this sliding. However, when a 2/1 laminate is bent with an uncured fibre prepreg in the middle, subsequently full-cured, and then unloaded, the metal layers are not able to spring-back independently anymore. In order to spring-back, the metal sheets should be unloaded elastically according to the stress distribution as sketched in Fig. 13(b). Besides, the two metal sheets are fixed after curing and the intermediate prepreg layer does not allow easy slip anymore, no spring-back can be feasible once the prepreg is full rigid. As a result, the spring-back can be greatly reduced and a larger residual stress remains at metal-prepreg interface. Due to the increase of second moment of area I and the curing of composite layer which resulting in a higher

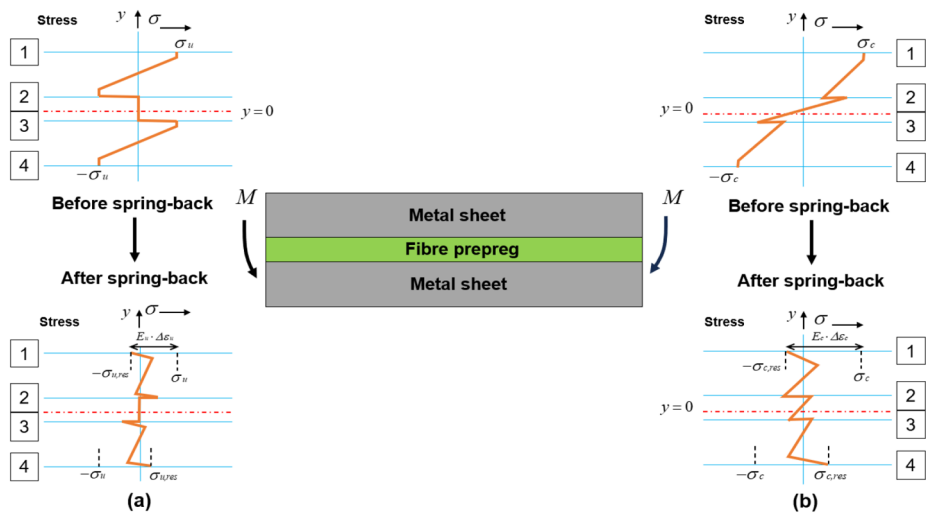


Fig. 13 Schematic diagram of stress distribution after bending for metal-composite laminates: **(a)** Bent with an uncured prepreg; **(b)** Bent with an uncured prepreg and subsequently full-cured

modulus from the state of uncured to full-cured, the unloading flexural stiffness E_C with a full-cured laminate is larger than the unloading flexural stiffness E_U with an uncured laminate. Therefore, with the gradual increase of residual stress during curing, the internal stress $\sigma_{C,RES}$ which related to the elastic strain recovery increases until the full-cured state. As the study focuses on the out-of-plane spring-back where the dominate parameters are the elastic energy versus total energy, the region for elastic deformation is reduced after full-cured which slows down the process of spring-back, as the schematic diagram shown in Fig. 14. In order to investigate the effect of the prepreg system on the spring-back after full-cured, cross-sectional micrographs on the central region of the laminate from the extracted profile (Fig. 10) are provided in Fig. 15. Various laminate structures after spring-back are presented and the prepreg layers are divided by the metal layers in the white areas. The nominal thickness for carbon fibre prepreg and glass fibre prepreg layer are 300 μm and 360 μm , and the average thickness of the prepreg layer drops to 205.67 μm and 278.46 μm , respectively, as shown in Fig. 15 (a) and (c). This demonstrates that the gradual curing process causes the matrix transverse flow and squeeze-out, which decreases the laminate thickness after curing.

The laminate layup and fibre orientation affect the overall thickness and the elastic modulus of the metal-composite laminates, which are also factors affecting the spring-back. Figure 16 exhibits the variations of the spring-back ratio after full-cured K_2 under various combinations of laminate layups and fibre orientations for the metal-composite laminates. The spring-back ratios after full-cured of the aluminium-based fibre metal laminates are between 0.09 and 0.15, while the ratios of spring-back are less than 0.08 when replacing the aluminium sheet to stainless steel in hybrid laminates. This further validates that the types and properties of the metal sheet influence the spring-back after full-cured of the laminates. Besides, it is found from the figure that the increase of laminate layups leads to a moderate decrease on the spring-back ratio K_2 under the same fibre orientation condition. This is mainly due to the increase of overall thickness and the growth of residual stress during the hot-pressing process. When the laminate changes from 2/1 structure to 3/2 structure

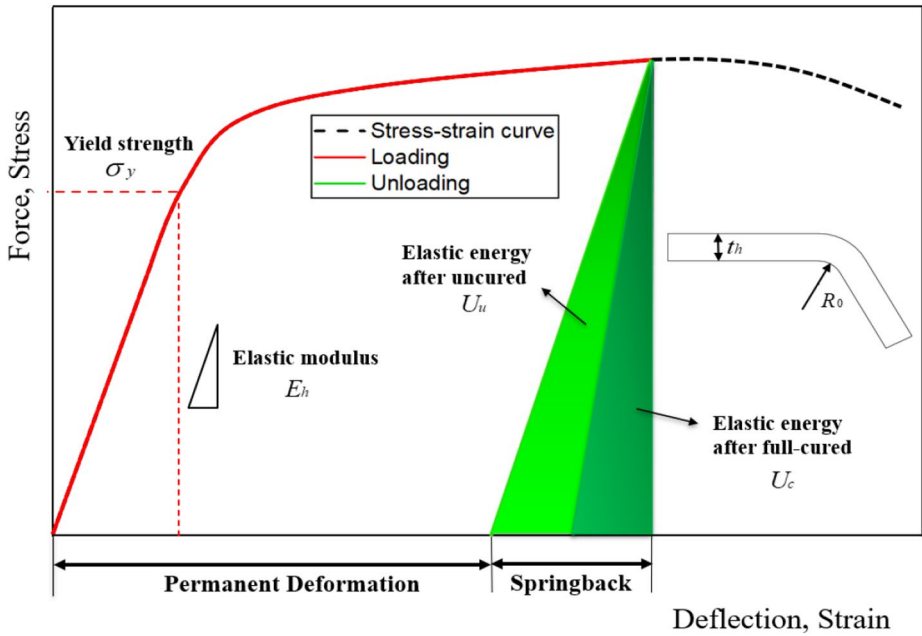


Fig. 14 Schematic diagram of the stress-strain response and spring-back analysis for metal-composite laminates

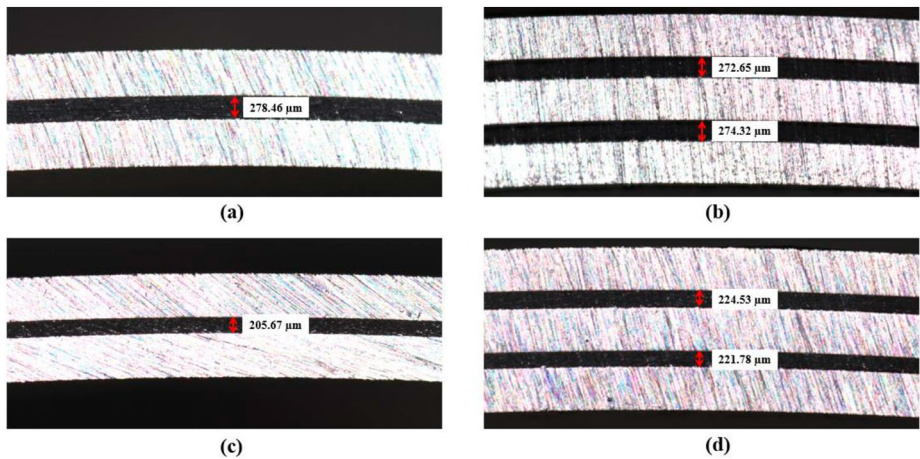


Fig. 15 Cross-sectional micrographs of the central region in hybrid laminates after full-cured process: (a) Al/GFRP with layup of 2/1 and fibre orientation of $0^\circ/0^\circ$; (b) Al/GFRP with layup of 3/2 and fibre orientation of $0^\circ/0^\circ$; (c) Al/CFRP with layup of 2/1 and fibre orientation of $0^\circ/0^\circ$; (d) Al/GFRP with layup of 3/2 and fibre orientation of $90^\circ/90^\circ$

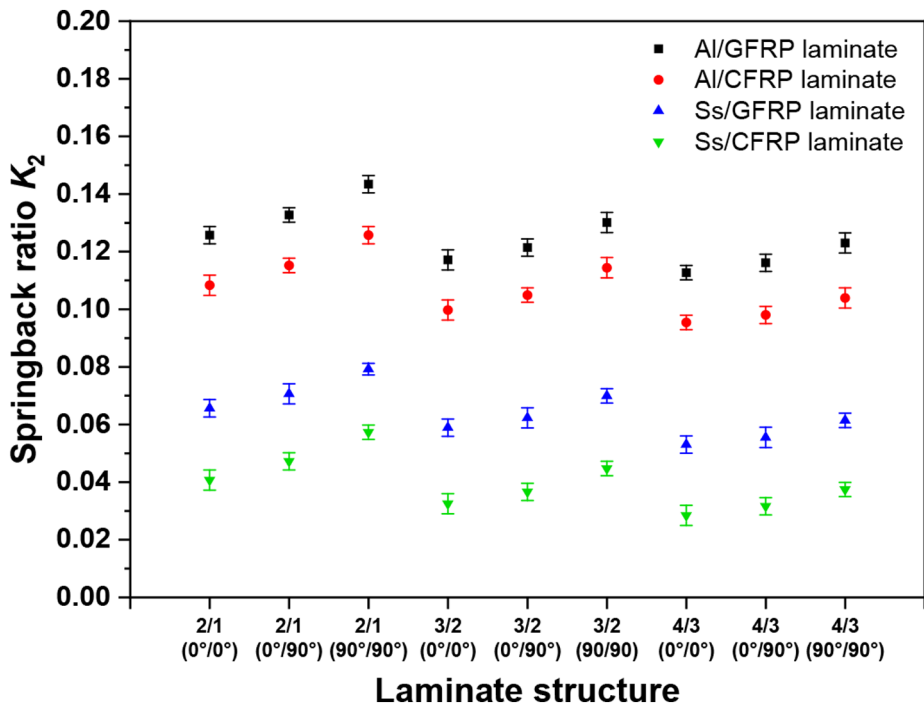


Fig. 16 Spring-back ratio K_2 under different layup and fibre orientation conditions for hybrid laminates

under the same fibre orientation and pressure conditions as shown in Fig. 15 (a) and (b), the prepreg thickness witnesses a slight decrease because of the stress redistribution with the increase of metal sheets. Although the prepreg thickness for each layer decreases, the overall thickness increases with the increasing number of layups. Therefore, as the radius/thickness ratio (R_0/t_h) affects the evolution of spring-back, the result follows the conclusion from the spring-back literatures of the metal sheet [15–17] where the increased thickness reduces the ratios of spring-back. Furthermore, the increase of prepreg layers promotes the growth of residual stresses which hinder the spring-back due to the increase of significant inelastic deformation. However, for metal-composite laminates with the same layups, the change of fibre orientation from $0^\circ/0^\circ$ to $90^\circ/90^\circ$ results in an increase on the spring-back after full-cured and there are mainly two reasons which can explain this phenomenon. First, the elastic modulus of the fibre prepreg is much lower than that of the metal sheet when the fibre orientation changes from 0° to 90° and consequently, the lower axial stress has less effect on the elastic unloading moment. Then, the epoxy in the prepreg with a fibre orientation of $90^\circ/90^\circ$ is more prone to squeeze out along the width direction during curing process, which largely reduces the prepreg thickness as well as the overall thickness. The cross-sectional micrographs shown in Fig. 15 (b)(d) validates the thickness reduction where the average prepreg thicknesses in 3/2 Al/GFRP laminate with a fibre orientation of $0^\circ/0^\circ$ and $90^\circ/90^\circ$ are $273.49 \mu\text{m}$ and $223.16 \mu\text{m}$, respectively. Therefore, the results on the fibre orientation effect further illustrates that the hybrid laminates with lower elastic modulus and lower thickness result in a larger spring-back ratio after full-cured.

3.3 Effect of Degree of Cure on Spring-Back

Throughout the hot-pressing process, forming temperature and holding time are two major parameters affecting the laminate spring-back and part quality. Therefore, various temperatures and times are set in the hot-pressing process to investigate the spring-back of the hybrid laminates after partially-cured under the forming pressure of 6 bar. Figure 17 exhibits the formed single-curved parts under three temperatures at the holding time of 20 min for Al/GFRP and Ss/CFRP laminate with a 2/1 layup and fibre orientation of $0^\circ/0^\circ$. Both hybrid materials show an increase in geometric depths with the increasing temperature for the optimum measure length while the tendency of growth is different. The geometric depth of the Al/GFRP laminate increases slightly when the temperature increases from 40°C to 80°C , but the increase is significant when the forming temperature reaches 120°C . However, the geometric depth for Ss/CFRP laminate undergoes a steady growth under these three temperatures. The observations illustrate that the increase of temperature results in the decrease of the partially-cured spring-back and the spring-back reduction is mainly due to the increase of elastic modulus resulting from increased crosslinking of the polymer network. Because the elastic modulus is higher, it requires larger residual stresses to cause the same amount of strain. Assuming that the spring-back of the metal sheet is consistent among the studied temperature range, the residual stresses generated by the glass fibre prepreg for Al/GFRP laminate before 80°C is too small to restrict the high spring-back behaviour of the aluminium sheet. However, when the forming temperature continues to rise, the higher residual stresses and friction in-between the layers greatly reduces the spring-back. For Ss/CFRP laminate, the spring-back of stainless steel itself is lower and the residual stress generated by the CFRP plays a smaller role on the elastic recovery of the laminate. Besides, the cross-section micrographs of the central region in the 2/1, $0^\circ/0^\circ$, Al/CFRP laminate under these temperatures and 20-minute holding time shown in Fig. 18 reveal that the average thickness of the prepreg decreases significantly from $273.94\text{ }\mu\text{m}$ to $212.63\text{ }\mu\text{m}$ as the temperature increases from 40°C to 120°C due to the epoxy squeeze flow and compaction along the width direction. The result demonstrates that the decrease of prepreg thickness for hybrid laminates has little effect on the partially-cured spring-back since the generation of residual stresses dominates the spring-back formation and lower the spring-back ratio.

The residual stress generated during the hot-pressing process depends on the reaction time of the epoxy system as well. Therefore, different holding times are proposed to study the time effect on the spring-back after partially-cured. Figure 19 presents the spring-back ratio K_1 of the Al/GFRP and Ss/CFRP laminates with the same 2/1 layup and fibre orientation of $0^\circ/0^\circ$ under various time and temperature conditions. When the holding time is zero, which denotes the instantaneous unloading as the pressure and temperature reach the set values, the spring-back ratio remains consistent within the studied range, and the Al/GFRP laminates even have layer separations at elevated temperature. As the time gradually increases, both laminates have a spring-back decreasing trend where higher holding time contributes to the decrease of spring-back. The trend can be explained by the evolution of degree of cure and degree of adhesion. When the epoxy system has no reaction time and zero degree of cure, the increase of forming temperature reduces the resin viscosity which decreases the degree of adhesion in-between the layers. The failure of layer separation occurs in the Al/GFRP laminate due to the higher spring-back behaviour of the aluminium alloy, while adhesion still occurs in the Ss/CFRP laminate even though the degree of adhe-

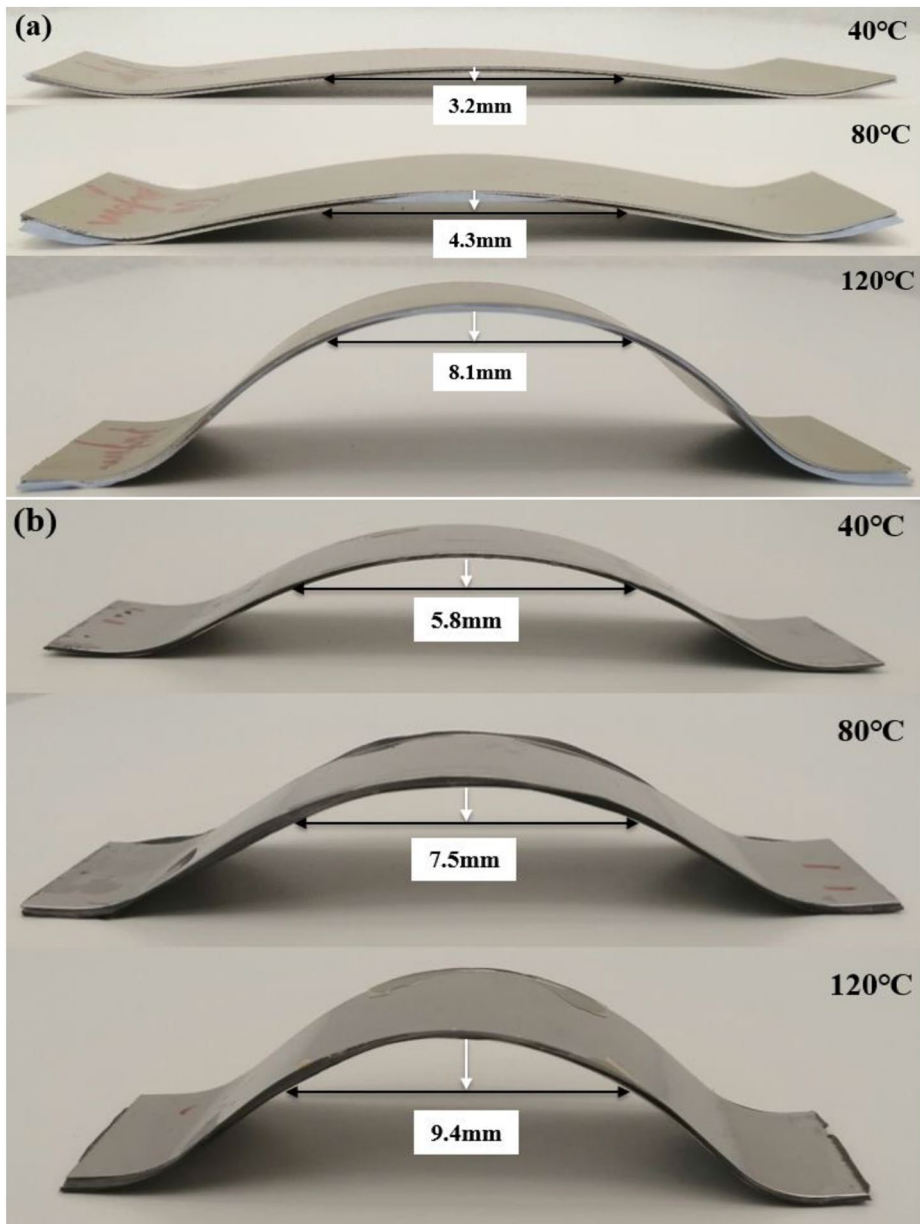


Fig. 17 Single-curved parts after spring-back for two metal-composite combinations under various temperatures at the holding time of 20 min: (a) 2/1, 0°/0°, Al/GFRP; (b) 2/1, 0°/0°, Ss/CFRP

sion is low at the temperature above 100°C. Once the holding time increases, the degree of cure and degree of adhesion increases, which hinder the release of elastic energy that has been accumulated in the laminate. In this case, there will be more interactions between the metal sheets and prepreg layers, and resulting in less spring-back and higher residual stress.

Fig. 18 Cross-section micrographs of the central region in 2/1, 0°/0°, Al/CFRP laminate under three temperature conditions

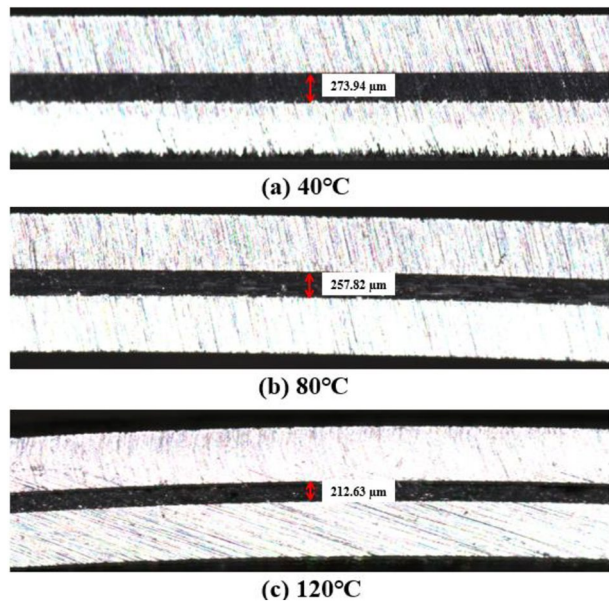


Figure 20 exhibits the evolution of the cure-dependent spring-back ratio K as a function of the degree of cure α for the metal-composite laminates. Here, the degree of cure for the spring-back after full-cured are set to be 0.9 and 0.95 for GFRP and CFRP materials, respectively and the computed values are obtained from Table 5. The figure reveals that hybrid laminates with the same prepreg system have similar trends of spring-back decreasing as the degree of cure increases. The spring-back ratios for the hybrid laminates drops significantly at the initial stage of curing, while the decrease becomes steady for metal/CFRP laminates at the degree of cure of 0.1 and the degree of cure of 0.4 for the metal/GFRP laminates. This indicates that metal sheets have limited influence on the partially-cured spring-back of the hybrid materials and the spring-back difference is mostly dependent on the thermos-chemical evolution of mechanical properties of the epoxy in prepreps.

3.4 Effect of Forming Pressure on spring-back

The results of the cure-dependent spring-back characterisation are all obtained under the forming pressure of 6 bar. However, the effect of forming pressure also plays a role on the spring-back behaviour of metal sheet and fibre prepreg. Figure 21 displays the spring-back ratio K_2 after full-cured under different pressure conditions for hybrid laminates with a 2/1 layup and fibre orientation of 0°/0°. It shows that the aluminium-based metal-composite combinations delaminate under low pressure conditions after curing, while the delamination disappears with the increase of pressure. The hybrid laminate with stainless steel does not delaminate at low pressure and the spring-back ratio after full-cured follows the trend where the value remains nearly constant at high pressure conditions. The trend shows that low forming pressure affects the final shape of the formed part and the increase of pressure above a certain level will not further improve the spring-back of the hybrid laminate at full-cured state. Even though the reduction of the overall thickness of the laminate once the

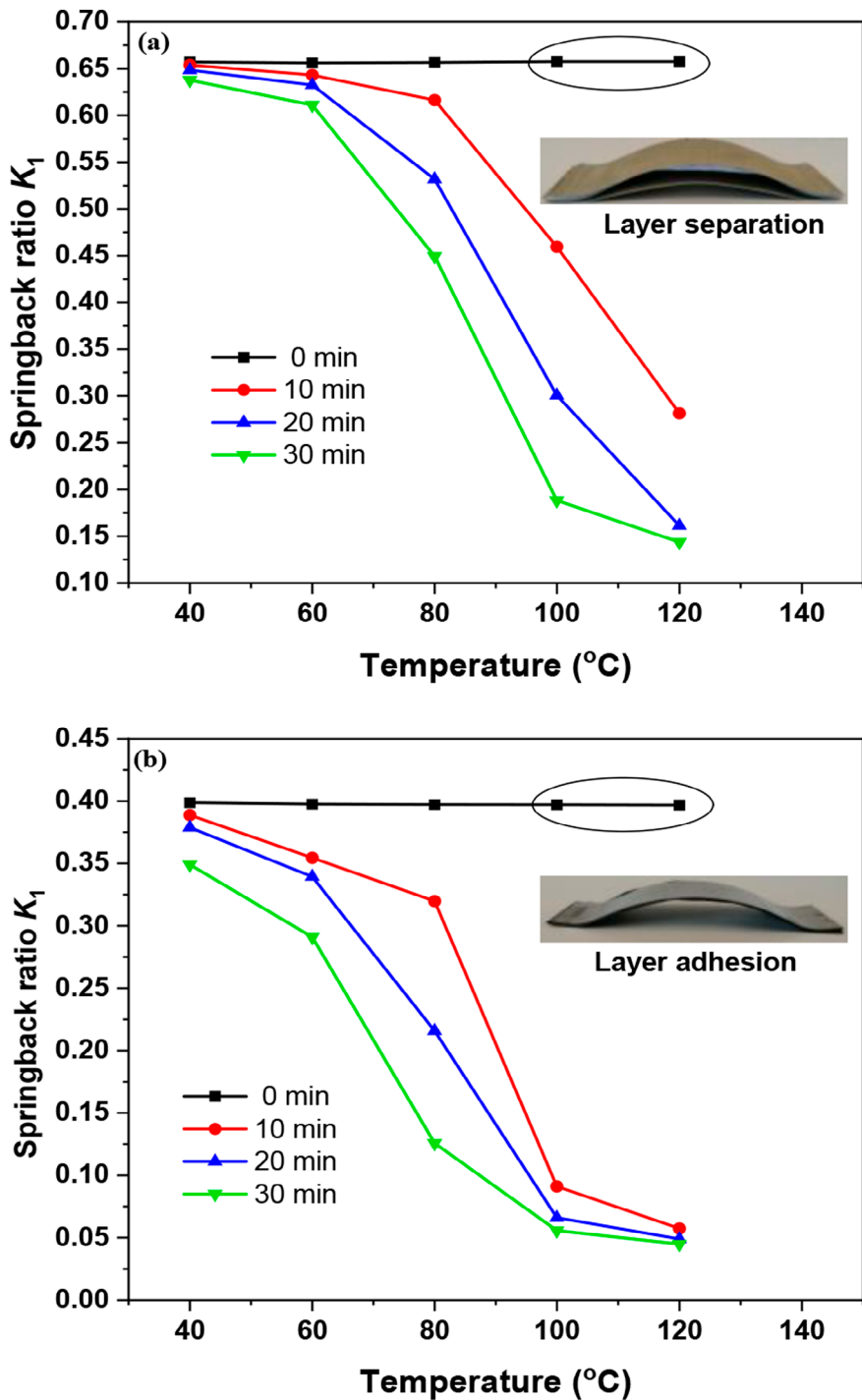


Fig. 19 Spring-back ratio K_1 under various temperature and time conditions after partially-cured process: (a) 2/1, $0^{\circ}/0^{\circ}$, Al/GFRP; (b) 2/1, $0^{\circ}/0^{\circ}$, Ss/CFRP

Fig. 20 Evolution of spring-back ratio K as a function of degree of cure α for metal-composite laminates

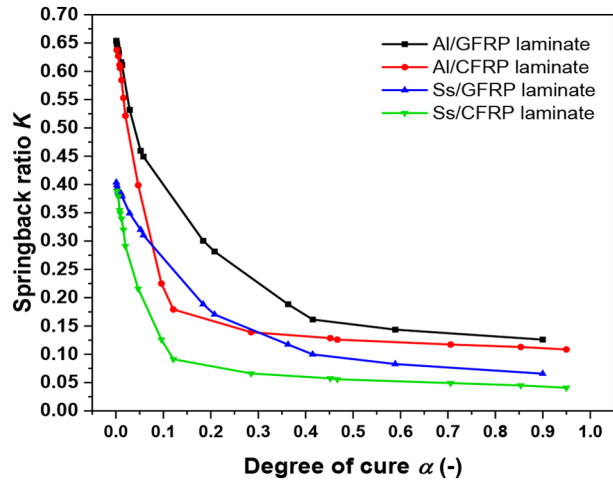
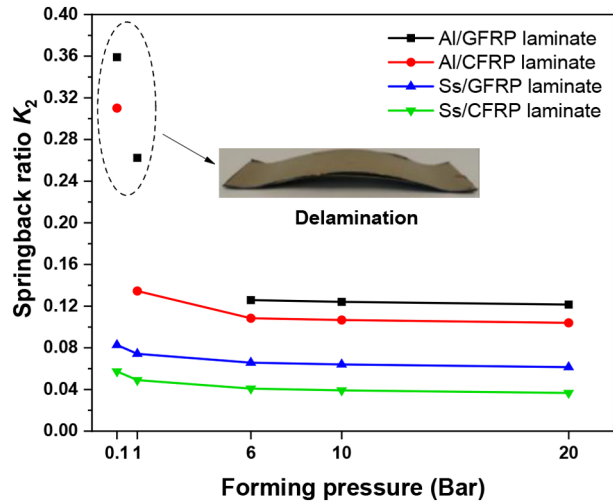


Fig. 21 Spring-back ratio K_2 after full-cured under different forming pressures for metal-composite laminates



pressure increases would somehow promote the spring-back, the increasing bending force between the metal sheet and prepreg layer results in the decrease of spring-back and higher residual stresses. The relative low degree of adhesion and friction under low pressure conditions is unable to compensate for the high elastic response of the aluminium alloy, which leads to the delamination after full-cured process. However, when the degree of cure and adhesion at the metal-prepreg interfaces reaches the maximum value for full-bonding, further increase of the pressure under curing conditions has limited effect on the spring-back. Therefore, the effect of forming pressure is negligible when the pressure reaches 6 bar during the hot-pressing process of metal-composite laminates.

4 Conclusions

The cure-dependent spring-back of metal-composite laminates is experimentally characterised during the hot-pressing process of a single-curved semi-cylindrical part. The spring-back ratios at the partially-cured and full-cured conditions are compared and the factors affecting the spring-back, including the material constituent, fibre orientation, laminate layup, holding time, forming temperature and pressure, are analysed in detail. The relevant conclusions are:

- (1) The irregular shape of a single-curved semi-cylindrical part with flange regions affects the evaluation of the spring-back behaviour for different material combinations. The formed radius at a measured length of 60 mm is considered to be the optimum length for accurate formed radius determination.
- (2) The cure-dependent spring-back and residual stress are counterparts. When the spring-back reduces because of the higher degree of cure, the residual stress increases and vice versa. They are both the result of the accumulated elastic energy and thermal effects in the laminate.
- (3) The spring-back of metal-composite laminates are mainly driven by the elastic modulus and yield strength of the metal constituent; the low elastic modulus as well as high yield strength as for the aluminium 2024-T3 shows more spring-back. The presence of prepreg system in the hybrid materials contributes significantly to the decrease of spring-back (by over 40%) when the laminate is full-cured. The increase of laminate layups results in a decrease of 1% on the full-cured spring-back, while the change of fibre orientation from 0°/0° to 90°/90° for the hybrid laminate witnesses an increase of 1–2% on the spring-back after full-cured.
- (4) The spring-back of the metal-composite laminates after partially-cured depends on the forming temperature and holding time during the hot-pressing process. The increase of degree of cure and degree of adhesion results in spring-back reduction of 50% for aluminium based hybrid laminates and 30% for stainless steel based hybrid laminates. Also, the decrease becomes steady for metal/CFRP laminates at the degree of cure of 0.1 and the degree of cure of 0.4 for the metal/GFRP laminates. The high spring-back characteristics of the aluminium alloy induces the failure of layer separation at low degree of cure levels.
- (5) The selection of forming pressure also influences the spring-back behaviour of hybrid laminates. The aluminium-based metal-composite laminate delaminates under low pressure conditions of less than 1kN after curing, while the delamination disappears with the increase of pressure. However, further increase of forming pressure has limited influence on the spring-back after full-cured and the pressure of 6 bar is regarded as a proper pressure for the hot-pressing of metal-composite laminates. Theoretical and experimental model incorporating the cure-dependent spring-back behaviour of the uncured hybrid laminates are needed to validate the results in the future.

Author Contributions All authors contribute to the study of concept and design. The first draft of the manuscript is written by Shichen Liu and all authors comment on the versions of the manuscript. All authors read and approve the final manuscript.

Funding The authors would like to thank the financial supports of China Scholarship Council (No.201906020174).

Data Availability No datasets were generated or analysed during the current study.

Declarations

Competing Interests The authors have no relevant financial or non-financial interests to disclose.

Open Access This article is licensed under a Creative Commons Attribution 4.0 International License, which permits use, sharing, adaptation, distribution and reproduction in any medium or format, as long as you give appropriate credit to the original author(s) and the source, provide a link to the Creative Commons licence, and indicate if changes were made. The images or other third party material in this article are included in the article's Creative Commons licence, unless indicated otherwise in a credit line to the material. If material is not included in the article's Creative Commons licence and your intended use is not permitted by statutory regulation or exceeds the permitted use, you will need to obtain permission directly from the copyright holder. To view a copy of this licence, visit <http://creativecommons.org/licenses/by/4.0/>.

References

1. Sinke, J.: Manufacturing of GLARE Parts and structures. *Appl. Compos. Mater.* **10**(4–5), 293–305 (2003). <https://doi.org/10.1023/A:1025589230710>
2. Sinmazcelik, T., Avcu, E., Bora, M., Çoban, O.: A review: Fibre metal laminates, background, bonding types and applied test methods. *Mater. Des.* **32**(7), 3671–3685 (2011). <https://doi.org/10.1016/j.matdes.2011.03.011>
3. Nardi, D., Abouhamzeh, M., Leonard, R., Sinke, J.: Investigation of kink induced defect in aluminium sheets for glare manufacturing. *Compos. Part. Appl. Sci. Manuf.* **125**(July), 105531 (2019). <https://doi.org/10.1016/j.compositesa.2019.105531>
4. Guo, Y., Zhai, C., Li, F., Zhu, X.: Formability, defects and strengthening effect of steel/CFRP structures fabricated by using the differential temperature forming process. *Compos. Struct.* **216**, 32–38 (2019). <https://doi.org/10.1016/j.compstruct.2019.01.106>
5. Kavitha, K., Vijayan, R., Sathishkumar, T.: Fibre-metal laminates: A review of reinforcement and formability characteristics. *Mater. Today Proc.* **22**, 601–605 (2020). <https://doi.org/10.1016/j.matpr.2019.08.232>
6. Mosse, L., Compston, P., Cantwell, W.J., Cardew-Hall, M.: The development of a finite element model for simulating the stamp forming of fibre-metal laminates. *Compos. Struct.* **75**(1–4), 298–304 (2006). <https://doi.org/10.1016/j.compstruct.2006.04.009>
7. Roth, S., Stoll, M., Weidenmann, K.A., Coutandin, S., Fleischer, J.: A new process route for the manufacturing of highly formed fiber-metal-laminates with elastomer interlayers (FMEL). *Int. J. Adv. Manuf. Technol.* **104**(1–4), 1293–1301 (2019). <https://doi.org/10.1007/s00170-019-04103-4>
8. Ding, Z., Wang, H., Luo, J., Li, N.: A review on forming technologies of fibre metal laminates. *Int. J. Light Mater. Manuf.* **4**(1), 110–126 (2021). <https://doi.org/10.1016/j.ijlmm.2020.06.006>
9. Heggemann, T., Homberg, W.: Deep drawing of fiber metal laminates for automotive lightweight structures. *Compos. Struct.* **216**, 53–57 (2019). <https://doi.org/10.1016/j.compstruct.2019.02.047>
10. Liu, S., Sinke, J., Dransfeld, C.: An inter-ply friction model for thermoset based fibre metal laminate in a hot-pressing process. *Compos. Part. B Eng.* **227**, 109400 (2021). <https://doi.org/10.1016/j.compositesb.2021.109400>
11. Chen, Q., Boisse, P., Park, C.H., Saouab, A.: Intra/inter-ply shear behaviors of continuous fiber reinforced thermoplastic composites in thermoforming processes. *Compos. Struct.* **93**(7), 1692–1703 (2011). <https://doi.org/10.1016/j.compstruct.2011.01.002>
12. Rashidi, A., Montazerian, H., Yesilcimen, K., Milani, A.S.: Experimental characterization of the interply shear behavior of dry and prepreg woven fabrics: Significance of mixed lubrication mode during thermoset composites processing. *Compos. Part. Appl. Sci. Manuf.* **129**, 105725 (2020). <https://doi.org/10.1016/j.compositesa.2019.105725>
13. Erland, S., Dodwell, T.J.: Quantifying inter- and intra-ply shear in the deformation of uncured composite laminates. *Adv. Manuf. Polym. Compos. Sci.* **7**(2), 25–35 (2021). <https://doi.org/10.1080/20550340.2021.1968190>

14. Shichen, L., Lihui, L., Shiwei, G.: An investigation into the formability and processes of GLARE materials using Hydro-bulging test. *Int. J. Precis Eng. Manuf.* **20**(1), 121–128 (2019). <https://doi.org/10.1007/s12541-019-00046-8>
15. Zhu, Y.X., Liu, Y.L., Yang, H.: Development and application of the material constitutive model in spring-back prediction of cold-bending. *Mater. Des.* **42**, 245–258 (2012). <https://doi.org/10.1016/j.matdes.2012.05.043>
16. Wagoner, R.H., Lim, H.: Advanced issues in spring-back. *Int. J. Plast.* **45**, 3–20 (2013). <https://doi.org/10.1016/j.ijplas.2012.08.006>
17. Wagoner, R.H., Wang, J.F.: Spring-back. *Metalwork. Sheet Form.* 733–755 (2018). <https://doi.org/10.31399/asm.hb.v14b.a0005131>
18. Chikalthankar, S.B., Belurkar, G.D., Nandedkar, V.M.: Factors affecting on spring-back in sheet metal bending: A review. *Int. J. Eng. Adv. Technol.* **3**(4), 247–251 (2014)
19. Sharad, G., Nandedkar, V.M.: Spring-back in sheet metal bending - a review. *J. Mech. Civ. Eng.* :53–56. (2015)
20. Shrivastava, P.: Study of spring-back process in sheet metal: A review. *Int. J. Res. Appl. Sci. Eng. Technol.* **8**(1), 222–226 (2020). <https://doi.org/10.22214/ijraset.2020.1040>
21. Sajan, M., Amirthalingam, M., Chakkingal, U.: A novel method for the spring-back analysis of a hot stamping steel. *J. Mater. Res. Technol.* **11**, 227–234 (2021). <https://doi.org/10.1016/j.jmrt.2021.01.017>
22. Wisnom, M.R., Gigliotti, M., Ersoy, N., Campbell, M., Potter, K.D.: Mechanisms generating residual stresses and distortion during manufacture of polymer-matrix composite structures. *Compos. Part. Appl. Sci. Manuf.* **37**(4), 522–529 (2006). <https://doi.org/10.1016/j.compositesa.2005.05.019>
23. Fiorina, M., Seman, A., Castanie, B., Ali, K.M., Schwob, C.: Spring-in prediction for carbon/epoxy aerospace composite structure. *Compos. Struct.* **168**, 739–745 (2017). <https://doi.org/10.1016/j.compstruct.2017.02.074>
24. Mezeix, L., Seman, A., Nasir, M.N.M., et al.: Spring-back simulation of unidirectional carbon/epoxy flat laminate composite manufactured through autoclave process. *Compos. Struct.* **124**, 196–205 (2015). <https://doi.org/10.1016/j.compstruct.2015.01.005>
25. Abouhamzeh, M., Sinke, J., Benedictus, R.: Prediction models for distortions and residual stresses in thermoset polymer laminates: An overview. *J. Manuf. Mater. Process.* **3**(4), 1–23 (2019). <https://doi.org/10.3390/jmmp3040087>
26. Brauner, C., Bauer, S., Herrmann, A.S.: Analysing process-induced deformation and stresses using a simulated manufacturing process for composite multispar flaps. *J. Compos. Mater.* **49**(4), 387–402 (2015). <https://doi.org/10.1177/0021998313519281>
27. Brauner, C., Frerich, T., Herrmann, A.S.: Cure-dependent thermomechanical modelling of the stress relaxation behaviour of composite materials during manufacturing. *J. Compos. Mater.* **51**(7), 877–898 (2017). <https://doi.org/10.1177/0021998316656924>
28. Uriya, Y., Yanagimoto, J.: Suitable structure of thermosetting CFRP sheet for cold/warm forming. *Int. J. Mater. Form.* **9**(2), 243–252 (2016). <https://doi.org/10.1007/s12289-015-1227-x>
29. Pereira, G.C., LeBoulluec, P., Lu, W.T., Yoshida, M.I.: Spring-back behavior on L-shaped composite structures: A statistical analysis of angular recovery as a function of time and residual cure. *Compos. Part. Appl. Sci. Manuf.* **124**, 105491 (2019). <https://doi.org/10.1016/j.compositesa.2019.105491>
30. Tarsha-Kurdi, K.E., Olivier, P.: Thermoviscoelastic analysis of residual curing stresses and the influence of autoclave pressure on these stresses in carbon/epoxy laminates. *Compos. Sci. Technol.* **62**(4), 559–565 (2002). [https://doi.org/10.1016/S0266-3538\(01\)00148-8](https://doi.org/10.1016/S0266-3538(01)00148-8)
31. Twigg, G., Poursartip, A., Fernlund, G.: Tool-part interaction in composites processing. Part I: Experimental investigation and analytical model. *Compos. Part. Appl. Sci. Manuf.* **35**(1), 121–133 (2004). [https://doi.org/10.1016/S1359-835X\(03\)00131-3](https://doi.org/10.1016/S1359-835X(03)00131-3)
32. Kravchenko, O.G., Kravchenko, S.G., Pipes, R.B.: Cure history dependence of residual deformation in a thermosetting laminate. *Compos. Part. Appl. Sci. Manuf.* **99**, 186–197 (2017). <https://doi.org/10.1016/j.compositesa.2017.04.006>
33. Guo, Y., Chen, Z.: Study on formability and failure modes of steel/CFRP based FMLs consisting of carbon fiber reinforced polymer prepreg and steel sheet. *Compos. Struct.* **281**, 114980 (2022). <https://doi.org/10.1016/j.compstruct.2021.114980>
34. Parsa, M.H., ahkami, S.N., al, Ettehad, M.: Experimental and finite element study on the spring-back of double curved aluminum /polypropylene/aluminum sandwich sheet. *Mater. Des.* **31**(9), 4174–4183 (2010). <https://doi.org/10.1016/j.matdes.2010.04.024>
35. Keipour, S., Gerdooei, M.: Spring-back behavior of fiber metal laminates in hat-shaped draw bending process: Experimental and numerical evaluation. *Int. J. Adv. Manuf. Technol.* **100**(5–8), 1755–1765 (2019). <https://doi.org/10.1007/s00170-018-2766-3>

36. Isiktas, A., Taskin, V.: Spring-back behavior of Fiber metal laminates with Carbon Fiber-Reinforced Core in V-Bending process. *Arab. J. Sci. Eng.* **45**(11), 9357–9366 (2020). <https://doi.org/10.1007/s13369-020-04796-w>
37. Hahn, M., Ben Khalifa, N., Weddeling, C.: Spring-back behavior of Carbon-Fiber-Reinforced Plastic Laminates with Metal Cover Layers in V-Die bending. *J. Manuf. Sci. Eng. Trans. ASME.* **138**(12), 1–8 (2016). <https://doi.org/10.1115/1.4034627>
38. Wang, J., Li, J., Fu, C., et al.: Study on influencing factors of bending spring-back for metal fiber laminates. *Compos. Struct.* **261**, 113558 (2021). <https://doi.org/10.1016/j.compstruct.2021.113558>
39. Kim, S.Y., Choi, W.J., Park, S.Y.: Spring-back characteristics of fiber metal laminate (GLARE) in brake forming process. *Int. J. Adv. Manuf. Technol.* **32**(5–6), 445–451 (2007). <https://doi.org/10.1007/s00170-005-0355-8>
40. Zal, V., Naeini, H.M., Bahramian, A.R., Sinke, J.: Investigation of the effect of temperature and layup on the press forming of polyvinyl chloride-based composite laminates and fiber metal laminates. *Int. J. Adv. Manuf. Technol.* **89**(1–4), 207–217 (2017). <https://doi.org/10.1007/s00170-016-9075-5>
41. Safari, M., Salamat-Talab, M., Abdollahzade, A., Akhavan-Safar, A.: Experimental investigation, statistical modeling and multi-objective optimization of creep age forming of fiber metal laminates. *Proc. Inst. Mech. Eng. Part. L J. Mater. Des. Appl.* **234**(11), 1389–1398 (2020). <https://doi.org/10.1177/1464420720943537>
42. Saadatfard, A., Gerdooei, M., Jalali Aghchai, A.: Drawing potential of fiber metal laminates in hydro-mechanical forming: A numerical and experimental study. *J. Sandw. Struct. Mater.* **22**(5), 1386–1403 (2020). <https://doi.org/10.1177/1099636218785208>
43. Blala, H., Lang, L., Khan, S., et al.: Forming Challenges of Small and Complex Fiber Metal Laminate Parts in Aerospace Applications—a Review, vol. 126. Springer London (2023). <https://doi.org/10.1007/s00170-023-11247-x>
44. Solvay Adhesive Materials: Technical Data Sheet FM- 94 Film Adhesive. <https://www.solvay.com/en/product/fm-94#product-documents>
45. Composites, S.H.D.: MTC510-UD epoxy prepreg datasheet. ;01:1–3. (2018). <https://shdcomposites.com/admin/resources/mtc510-tds.pdf>
46. Hardis, R., Peters, F.E., Kessler, M.R.: Cure kinetics characterization and monitoring of an epoxy resin using DSC, Raman spectroscopy, and DEA. *Compos. Part. Appl. Sci. Manuf.* **49**, 100–108 (2013). <https://doi.org/10.1016/j.compositesa.2013.01.021>
47. Abouhamzeh, M., Sinke, J., Benedictus, R.: Kinetic and thermo-viscoelastic characterisation of the epoxy adhesive in GLARE. *Compos. Struct.* **124**, 19–28 (2015). <https://doi.org/10.1016/j.compstruct.2014.12.069>
48. Sourour, S., Kamal, M.R.: Differential scanning calorimetry of epoxy cure: Isothermal cure kinetics. *Thermochim Acta.* **14**(1–2), 41–59 (1976). [https://doi.org/10.1016/0040-6031\(76\)80056-1](https://doi.org/10.1016/0040-6031(76)80056-1)
49. Dimopoulos, A., Skordos, A.: Cure kinetics, glass transition temperature development, and dielectric spectroscopy of a low temperature cure epoxy/amine system. *J. Appl. Polym. Sci.* **124**(3), 1899–1905 (2012). <https://doi.org/10.1002/app.34605>
50. Liu, J., Xue, W.: Unconstrained bending and spring-back behaviors of aluminum-polymer sandwich sheets. *Int. J. Adv. Manuf. Technol.* **91**(5–8), 1517–1529 (2017). <https://doi.org/10.1007/s00170-016-9819-2>

Publisher's Note Springer Nature remains neutral with regard to jurisdictional claims in published maps and institutional affiliations.